characterize visco-elastic polymers (*16*), appear to be necessary to define turbulent behavior of suspensions of interacting particles.

NOTATION

D = pipe inside diameter, ft.
du/dr = shear rate
g_c = conversion constant, 32.2 lb._m ft./lb._f sec.^{2}
K = Ostwald-deWaele coefficient, lb._f/sq.ft.-sec.^{n}
L = axial distance, ft.
n = Ostwald-deWaele exponent

Greek Letters

ΔP = pressure drop, lb._f/sq.ft.
η = Bingham plastic coefficient of rigidity, lb._m/ft.-sec.
μ = wall shear stress viscosity, lb._m/ft.-sec.
μ_D = viscosity of dispersed suspension, lb._m/ft.-sec.
μ_s = specific viscosity, ratio of dispersed viscosity to water viscosity at the same temperature
μ_w = water viscosity, (lb._m/ft.-sec.)
ρ = density of suspension, lb._m/cu. ft.
τ = shear stress, lb._f/sq.ft.
τ_w = wall shear stress $D\Delta P/4L$, lb._f/sq.ft.
τ_y = Bingham plastic yield stress, lb._f/sq.ft.

LITERATURE CITED

1. Dodge, D. W., and A. B. Metzner, *A.I.Ch.E. Journal*, **5**, 189 (1959).
2. Shaver, R. G., and E. W. Merrill, *ibid.*, p. 181.
3. Caldwell, D. H., and H. E. Babbitt, *Trans. Am. Inst. Chem. Engrs.*, **37**, 237 (1941); *Ind. Eng. Chem.*, **33**, 249 (1941).
4. Weltmann, R. N., *Ind. Eng. Chem.*, **48**, 386 (1956).
5. Thomas, D. G., *A.I.Ch.E. Journal*, **6**, 631 (1960).
6. Hedstrom, B. O. A., *Ind. Eng. Chem.*, **44**, 561 (1952).
7. Bogue, D. C., Ph.D. thesis, University of Delaware, Newark, Delaware (1960).
8. Rabinowitch, B., *Z. Phys. Chem.*, **A145**, 1 (1929).
9. Eissenberg, D. M., "Developments in Theoretical and Applied Mechanics," Vol. 1, Plenum Press, New York (1963).
10. Lane, J. A., et al., "Fluid Fuel Reactors," p. 162, Addison Wesley, Reading, Pennsylvania (1958).
11. Johnsson, K. O., and R. H. Winget, *USAEC Report ORNL-2853*, Oak Ridge National Laboratory, Oak Ridge, Tennessee (Dec. 8, 1959).
12. Eissenberg, D. M., *USAEC Report ORNL-3233*, Oak Ridge National Laboratory, Oak Ridge, Tennessee (Feb. 28, 1962).
13. Moody, L. F., *Trans. Am. Soc. Mech. Engrs.*, **66**, 672 (1944).
14. Wilson, J., *Trans. Am. Soc. Civil Engrs.*, **107**, 1576 (1942).
15. Eissenberg, D. M., unpublished data.
16. Ferry, J. D., "Viscoelastic Properties of Polymers," Wiley, New York (1961).

Manuscript received June 27, 1963; revision received October 25, 1963; paper accepted October 25, 1963.

Thermodynamic Comparison of Large-Scale Liquefaction of Air, Hydrogen, and Helium

R. E. LATIMER and R. A. MOSTELLO
American Cryogenics, Incorporated, O'Fallon, Illinois

In the United States in the 1940's, liquefaction of air was achieved on the large scale of millions of standard cubic feet per hour or thousands of tons per day of liquid products. This consisted of production primarily of liquid oxygen and to a lesser extent of liquid nitrogen and liquid argon. These were stored, transported, and used in some cases as liquid.

Two decades later in the United States, in the 1960's, hydrogen will be liquefied on the large scale of millions of standard cubic feet per hour. This is hundreds of tons per day of liquid hydrogen. This liquid hydrogen will be burned with liquid oxygen in National Aeronautics and Space Administration rockets for the exploration of space.

Oxygen and hydrogen are among the most reactive of chemical substances and are unlimited in their availability. This is not true of helium. However, it does not seem unreasonable to guess that re-liquefaction of helium, primarily for deep refrigeration purposes, will also be carried out on the large scale of millions of standard cubic feet per hour in the United States in the 1980's. This is hundreds of tons per day of helium liquefaction.

Efficient large-scale liquefaction of air or hydrogen or helium requires the expenditure of 2 to 4 kw. per 100 std. cu. ft./hr., and so a production level in the United States of millions of standard cubic feet per hour of any of these liquefied gases requires the expenditure of tens of thousands of kilowatts. The investment in gas compressors is millions of dollars, and the annual power cost is millions of dollars for such a scale of liquefaction.

This paper examines the problem of minimizing the power consumption for liquefaction and thus reducing the high cost of power, of compressors, and of other plant investment.

LOGARITHMIC REPRESENTATION

When certain physical properties of various fluids are represented on a logarithmic graph of temperature vs. pressure, or on a graph of the property vs. log pressure or log temperature and with families of curves at similar reduced temperature or pressure, the curves are of similar shape for the different fluids but are at different locations on the graph. Logarithmic scales of temperature and

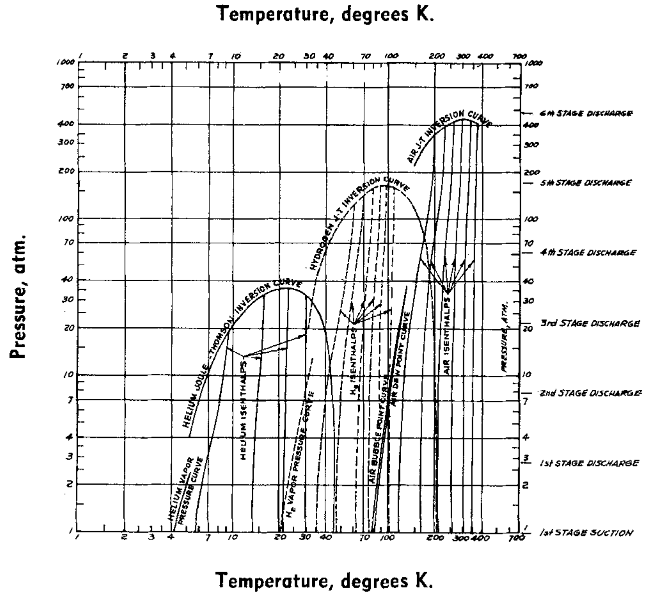

Fig. 1. Joule-Thomson inversion curves, vapor pressure curves, and vapor isenthalps.

pressure place equal emphasis on properties of each fluid regardless of relative position on the absolute temperature scale. Curves for different fluids are offset from each other rather than coincident as they would be on reduced properties plots, but their similar shapes are to be expected from the law of corresponding states.

In cryogenic processes, boiling Freons are the precoolants for high-pressure air or nitrogen, boiling nitrogen is the precoolant for high-pressure hydrogen, and boiling hydrogen is the precoolant for medium-pressure helium. The triple point of nitrogen at 63.1°K. and 2 lb./sq.in.abs. and the triple point of hydrogen at about 13.9°K. and 1 lb./sq.in.abs. impose a practical limitation on how low a precooling temperature can be reached by vacuum-pumping the liquid precoolant without solidifying it. Hydrogen precoolant for helium has been vacuum-pumped to 10°K. and 0.04 lb./sq.in.abs., which is well down into the solid hydrogen region, in Simon batch type of laboratory-scale liquefiers (reference *16*, pp. 64 to 67). However, this would not be a satisfactory method of operation for a large-scale liquefier.

Figure 1 shows the Joule-Thomson inversion curves for air (*10*), hydrogen (*19*), and helium (*8*), on a graph of log pressure vs. the logarithm of the absolute temperature. The vapor pressure curves appear for reference. At any point on the inversion curve, a small reduction in pressure through a throttling valve is accompanied by no reduction or rise in temperature. At the temperature reached by precooling, the inversion pressure is the one at which the high-pressure gas will have the lowest enthalpy when it enters the warm end of the main heat exchanger of the gas liquefier. On Figure 1, constant enthalpy lines, extending from the inversion curve down to atmospheric pressure, are shown for each fluid. This shows the number of degrees of Joule-Thomson cooling achieved on expansion through a valve by starting from any precooled condition. The high-pressure expansion valve is at the cold end of the main heat exchanger, but one should examine the enthalpy relationships of the individual streams at the warm end of the heat exchanger to understand the refrigeration capability of a liquefier.

The stages of compression at equal pressure ratios are equal distances on a logarithmic pressure scale. Figures 1, 2, 3, and 4 show the discharge pressures based on a pressure ratio of 2.8 for each successive stage of compression. Each stage of compression at equal pressure ratio and equal initial temperature requires equal power and is an equal distance on the scale of the logarithm of the pressure. The scale of log pressure is in this case, therefore, a direct measure of the compression energy per standard cubic foot of gas. Each increment of log pressure for an expansion engine represents an equal increment of engine work removed, divided by the absolute temperature. Thus the logarithmic pressure scale shows the refrigeration value of each increment of an engine expansion because the refrigeration value is approximately the number of B.t.u.'s removed, divided by the absolute temperature.

JOULE-THOMSON REFRIGERATION

Since the scope of this paper is limited to large-scale liquefaction, attention is focused on minimizing the power consumption rather than on matters of convenience and simplicity such as avoiding the complexity and hazards of hydrogen liquefaction for the precooling of helium and the hazards of using high pressure. Minimized power consumption requires using high pressure to obtain maximum Joule-Thomson refrigeration per unit of compressor power, using precoolants to increase the Joule-Thomson effect, and using expansion engines to cool by external work the part of the high-pressure gas that is in excess of the amount that can be fully cooled countercurrent to the unliquefied gas being rewarmed.

Figures 2, 3, and 4, introduce, for air, hydrogen, and helium respectively, the thermodynamic function $(\partial H/\partial \ln P)_T$; that is, the amount of change in enthalpy per increment of log pressure (or per increment of compressor work) at constant precool temperature. This function is plotted vs. log pressure. Each figure shows curves for three different temperatures to which the high-pressure gas might be precooled. The height of the curve shows the amount of Joule-Thomson refrigeration available from each increment of compression. The area under the curve from one pressure to another is the amount of Joule-Thomson refrigeration that is obtained with a liquefaction cycle in which the compressor operates between these two pressures and the fluid is precooled to the temperature that the curve represents.

A convenient pressure ratio for each stage of an air compressor is 2.8, and ln 2.8 minus ln 1.0 is numerically equal to 1.03, or nearly unity. Therefore, on Figures 2, 3, and 4, the area under a curve spanning one such stage of

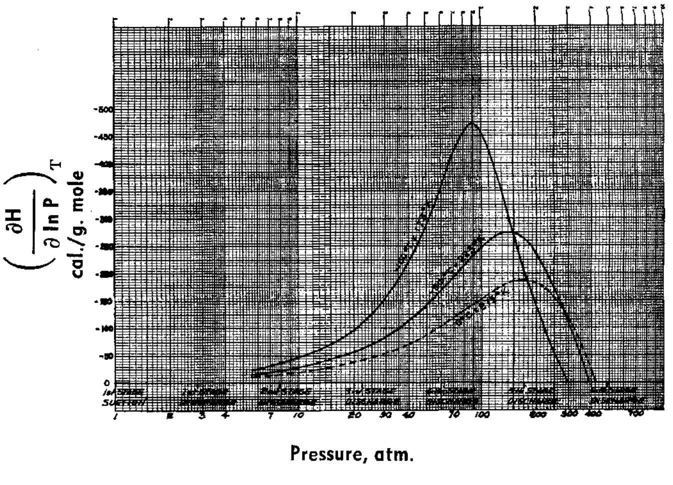

Fig. 2. $(\partial H/\partial \ln P)_T$, isotherms for air.

compression is numerically almost equal to the average height of the curve over that range.

Figure 2, for air, shows that the fifth stage of compression produces much more Joule-Thomson refrigeration value than any other stage. This is the compression from 62 atm. to 173 atm. With precooling to 0°C. (273°K.), the fifth stage produces about 160 cal. of Joule-Thomson refrigeration per gram mole of air compressed (290 B.t.u./lb. mole). Each pound molecular weight of any gas occupies 387 std. cu. ft. at standard conditions of 70°F. and 1 atm. absolute. Thus, by precooling with the aid of Freon to 0°C., the fifth stage of air compression from 62 to 173 atm. has a Joule-Thomson refrigeration value of 290 B.t.u. per 387 std. cu. ft. of air compressed.

However, if Freon precooling to −50°C. (223°K.) is used, the fifth stage of air compression produces about 250 cal./g. mole (450 B.t.u./387 std. cu. ft.) of Joule-Thomson refrigeration. If precooling with Freon 13 to −100°C. (173°K.) is done, the Joule-Thomson refrigeration produced by the fifth stage of air compression is about 390 cal./g. mole (700 B.t.u./387 std. cu. ft.) of air. Thus, deep precooling of the high-pressure air is very valuable in increasing the fraction of the air liquefied by the process.

As Figure 2 shows, each successive stage of air compression up to the fifth stage makes substantially more Joule-Thomson refrigeration than the preceding stage of compression. Therefore, to minimize power consumption in liquefaction, one might consider an air or nitrogen refrigeration cycle which operates from 22 atm. up to 173 atm., or from 8 atm. up to 173 atm. The lower stages of compression are not as useful.

When one considers the above-mentioned figures of 290 or 450 or 700 B.t.u. of Joule-Thomson refrigeration per 387 std. cu. ft. of air from the fifth stage of compression, using precooling to 0°, −50°, or −100°C., respectively, *it is significant to compare refrigeration losses* and expansion engine refrigeration. A 200-ton/day air-separation and liquefaction plant is likely to have an incoming heat leak of about 0.9 B.t.u./lb. of high-pressure air, or about 26 B.t.u./387 std. cu. ft. With a temperature difference of 15°F. between the high-pressure air entering the warm end of the main heat exchanger after precooling and the unliquefied low-pressure air or waste nitrogen leaving the warm end of the main heat exchanger (about 75% of the high-pressure air entering), there is a loss of 15 × 7 × 0.75, or 79 B.t.u. refrigeration per 387 std. cu. ft. of high-pressure air.

A 77%-efficient engine which expands 60% of the high-pressure air from 189 atm. and 228°K. down to 10 atm. and saturation (108°K.), removes 34 B.t.u./lb. of air expanded, or 590 B.t.u./387 std. cu. ft. of total high-pressure air. This is an engine expansion spanning the third, fourth, and fifth stages of compression.

Figure 3 shows in similar fashion the decrease in enthalpy of high-pressure hydrogen at various precool temperatures of 80°, 69°, and 64°K. achieved by boiling of nitrogen, per increment of log pressure or per increment of compressor work. Precooling to 80°K. requires the boiling of nitrogen at 20 lb./sq.in.abs. Precooling to 69°K. requires vacuum-pumping of the nitrogen to 5 lb./sq.in. abs. Precooling to 64°K. requires vacuum-pumping the nitrogen to 2 lb./sq.in.abs. Lower precooling temperature is accompanied by more area under the curve in Figure

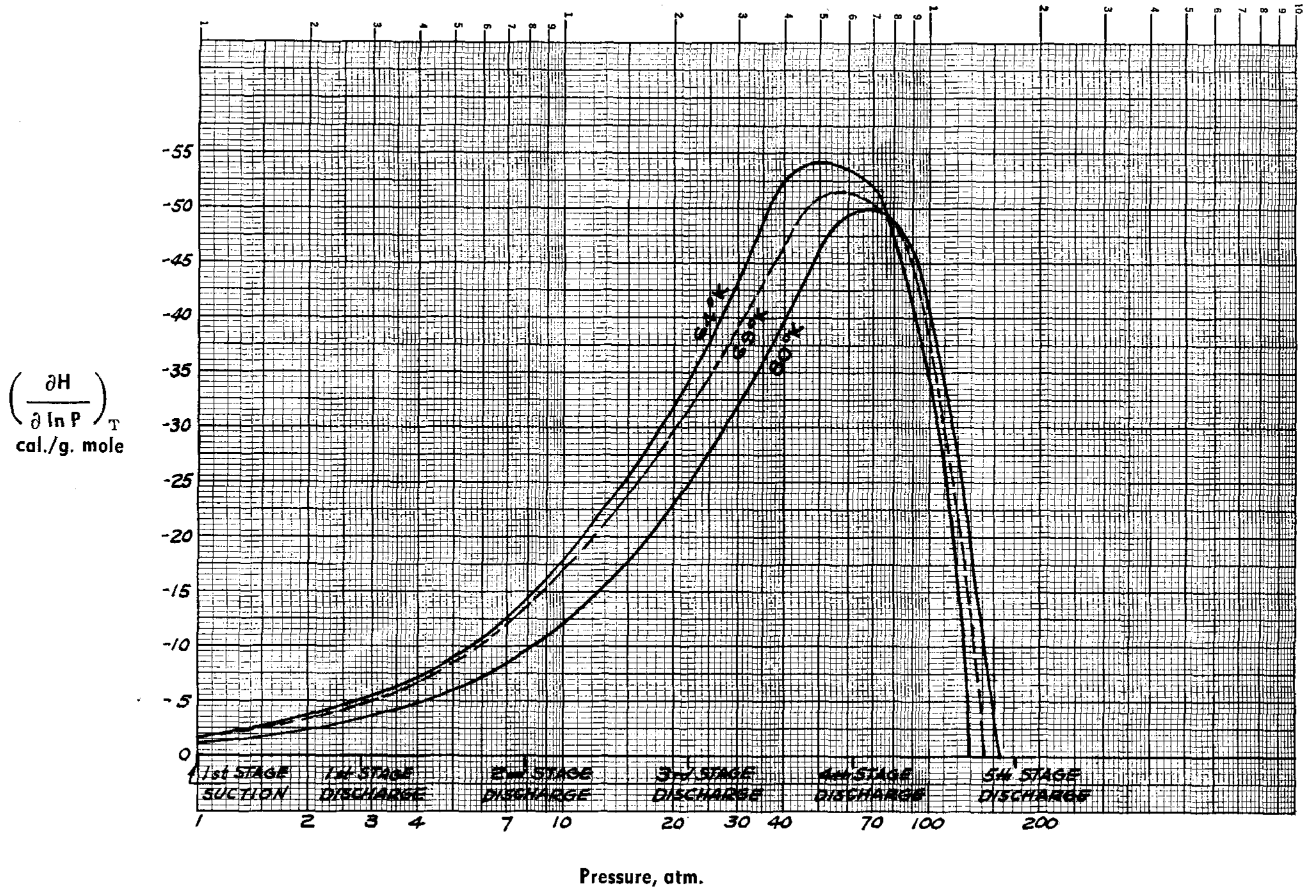

Fig. 3. $(\partial H/\partial \ln P)_T$, isotherms for hydrogen.

3, and thus more Joule-Thomson refrigeration is developed between any hydrogen compressor intake and discharge pressures.

Figure 4 shows for helium the decrease in enthalpy of medium pressure helium per increment of log pressure or per increment of compressor work, with precooling to 22°, 14°, or 11°K., respectively, by boiling of hydrogen. Precooling to 22°K. requires boiling of hydrogen at 23 lb./sq.in.abs. Precooling to 14°K. requires vacuum-pumping of hydrogen to 1.1 lb./sq.in.abs. Precooling to 11°K. requires vacuum-pumping of solid hydrogen far below the triple point, to 0.1 lb./sq.in.abs. Figure 4 shows clearly that precooling by vacuum-pumping nearly to 14°K. is quite important, and that vacuum-pumping of the solid hydrogen almost to 11°K. might be advantageous if it were mechanically practical.

It became apparent to us in the study of liquefaction processes over the extreme temperature range from Freon evaporators down to helium liquefaction, that heat-exchanger temperature differences must be kept down approximately in proportion to the absolute temperature. This is inherent in the second law of thermodynamics, and it appears plausible when processes are examined on graphs utilizing logarithmic representation of the absolute temperature. We have chosen to design heat exchangers for temperature differences of about 0.036 times the absolute temperature. This is an arbitrary figure which is in approximate agreement with main heat exchangers which are generally in use in large air liquefaction plants. This is about 8°C. at the 230°K. level, 2.5°C. at the 69°K. level, 0.5°C. at the 14°K. level, and 0.15°C. at the 4.2°K. level. In some cases, heat-exchanger temperature differences pinch out almost to zero at an intermediate point and unavoidably open up to much larger differences at the cold end and the warm end.

MINIMUM CARNOT WORK REQUIREMENTS FOR LIQUEFACTION

Figure 5 shows the amount of sensible heat that must be removed, as well as the latent heat of liquefaction, in cooling down at atmospheric pressure from a sink temperature of 302.6°K. (85°F.). The amount of cumulative heat removal is shown plotted vs. temperature for air liquefaction, for helium liquefaction, for hydrogen cooling, ortho to para conversion, and liquefaction. The solid line for hydrogen is based on catalyzed continuous ortho to para conversion during cool-down. This basis was chosen in order to remove heat at as high a temperature as possible. The dashed line for hydrogen shows all the ortho to para conversion done after cool-down to the liquefaction temperature of 20°K. In the case of helium, the negligible latent heat compared to the sensible heat should be noted. This is why a helium liquefier requires far more power than a helium refrigerator which has only latent heat to remove. Figure 5 is based entirely on sensible and latent heat removal at 1 atm. pressure.

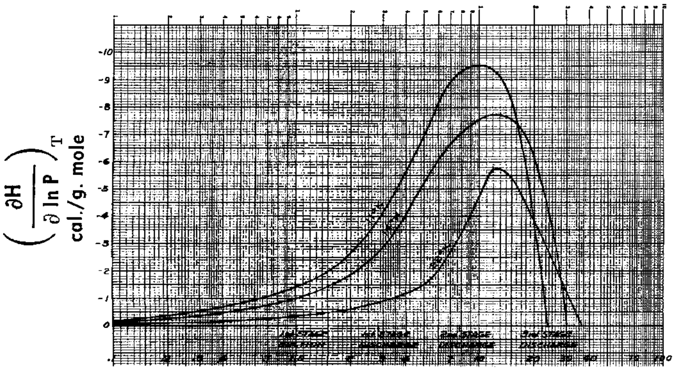

Fig. 4. $(\partial H/\partial \ln P)_T$, isotherms for helium.

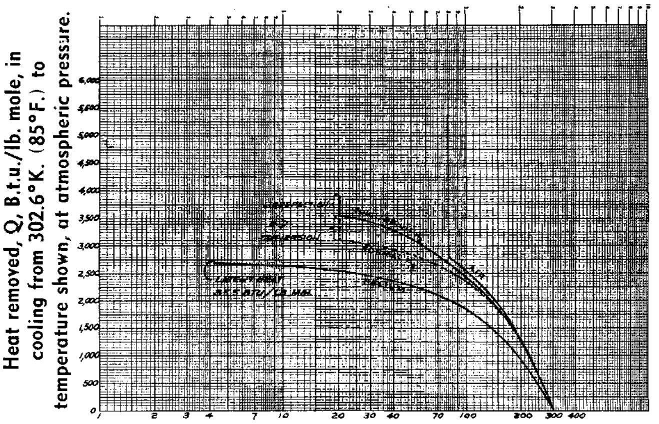

Fig. 5. Cumulative heat-removal cooling curves.

Figure 6 shows the minimum Carnot work required to pump to the sink temperature the heat that must be removed at each temperature level if the gas to be liquefied is cooled at atmospheric pressure (as on Figure 5). That a much greater proportion of work is required to remove heat for latent heat removal at the lowest temperature level than for sensible heat removal at higher temperatures up to the sink temperature may be seen by a comparison of Figures 5 and 6. Figure 6 shows cumulatively the work requirement down to each successive temperature level. The minimum work for hydrogen liquefaction is shown to be 36% greater if the ortho to para conversion is all done at liquefaction temperature rather than if an equilibrium is maintained during the cool-down.

For air, not quite half of the heat removed is latent heat, but over three-fourths of the Carnot work is for the latent heat removal. For hydrogen, less than one-tenth of the heat removed is heat of liquefaction, and one-ninth is heat of ortho to para conversion. Because of the low temperature level of the liquefaction, nearly half of the Carnot work for hydrogen is for the liquefaction, and about one-seventh is for continuous equilibrium ortho to para conversion. For helium, only 1.3% of the heat removed is latent heat (35.5 B.t.u./lb. mole), but since this is at the lowest temperature level it requires 22% of the total work. Thus, a helium refrigerator requires only about 22% as much power consumption for reliquefying cold helium as that which is required for liquefying helium gas initially at ambient temperature. A helium refrigerator requires that the gas be warmed to ambient temperature, compressed, and then cooled again. However, the object is to remove latent heat from the cold gas.

The Carnot work requirement per increment of heat removal at each temperature level is shown by means of the top curve on Figure 7. This is based on the simple equation

$$\frac{W}{Q} = \frac{T_s - T}{T}$$

or in differential form

$$\frac{dW}{dQ} = \frac{T_s - T}{T}$$

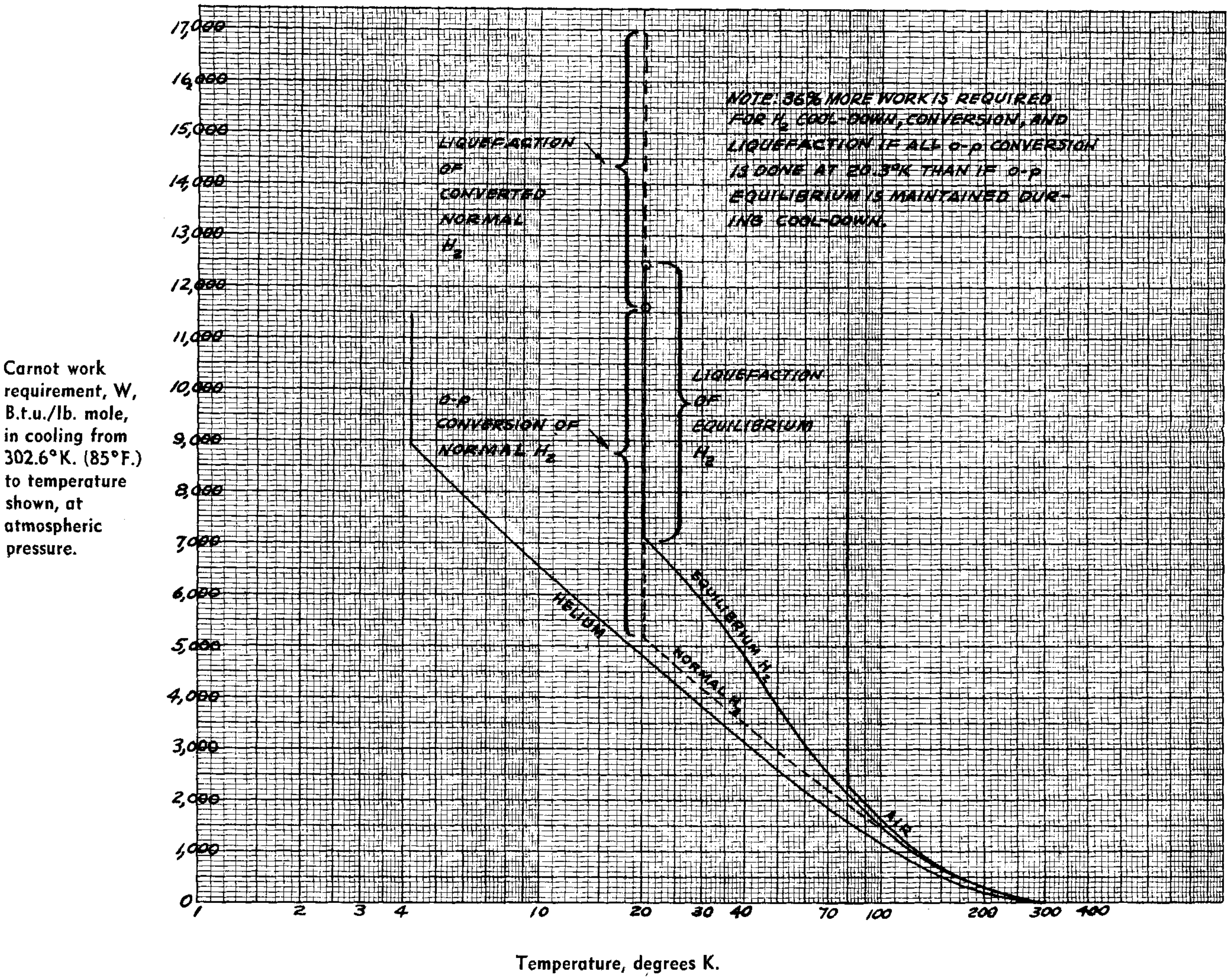

NOTE: 36% MORE WORK IS REQUIRED FOR H_2 COOL-DOWN, CONVERSION, AND LIQUEFACTION IF ALL o-p CONVERSION IS DONE AT 20.3°K THAN IF o-p EQUILIBRIUM IS MAINTAINED DURING COOL-DOWN.

Fig. 6. Cumulative Carnot-work cooling curves.

in which T_s is the sink temperature of 302.6°K. (85°F.), and T is the absolute temperature (in degrees Kelvin) at which the heat is removed and pumped to the sink temperature. At air liquefaction temperature of about 80°K., the work required is 2.8 times the heat removed. At hydrogen liquefaction temperature of 20°K., the work is 14 times the heat removed. At helium liquefaction temperature of 4.2°K., the work is 72 times the heat removed. At absolute zero, of course, infinite work is required to remove 1 B.t.u. of heat, but fortunately the specific heat of materials approaches zero at this point so that cooling of materials nearly to absolute zero is not quite as tremendous a task as it would be otherwise. The differential form of the above equation should be used if the heat, Q, is absorbed over a range of temperature so that T varies, as is the case for sensible heat removal (Figure 5).

The lower curves of Figure 7 show the ratio of the cumulative Carnot work during cool-down (from Figure 6) divided by the cumulative heat removal during cool-down (from Figure 5), plotted vs. temperature. Separate curves are shown for air, for helium, for hydrogen with continuous equilibrium ortho to para conversion, and for hydrogen with the ortho to para conversion done entirely at liquefaction temperature. It is interesting that for cooling and liquefaction of helium only 4.2 times as much Carnot work is required as the total heat removed, even though for the latent heat removal at the lowest temperature level 72 times as much work is required as the heat which it removes. If the ortho to para conversion of hydrogen is carried out during cool-down, a total of 3.1 times as much Carnot work is required for hydrogen cool-

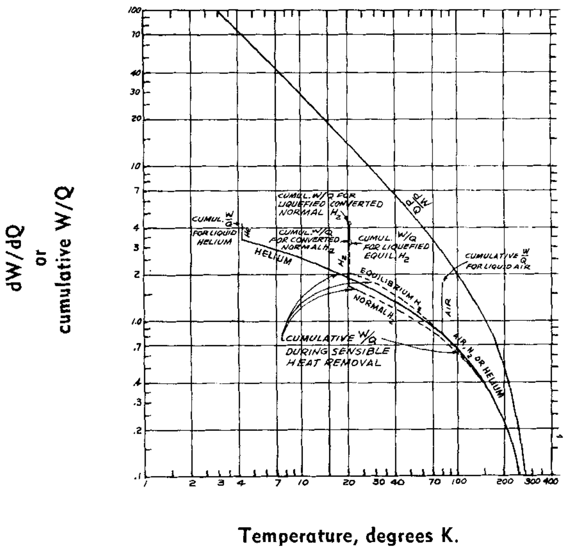

Fig. 7. Cumulative Carnot-work/heat-removal cooling curves.

TABLE 1. POWER REQUIREMENTS OF LIQUEFACTION PROCESSES

Gas liquefied	Air	Air	Air	Air	H_2	H_2	H_2	Helium	Helium
Temp. liquefied at, °K.	83	83	83	83	20.3	20.3	20.3	4.22	4.22
°C.	—190	—190	—190	—190					
Precool temp., °K.	249	228	189	169	80	69	64	14	11
°F.	—12	—50	—120	—156					
Max. pressure compressed to, atm.	307	194	358	166	148	133	123	28.5	24
% of high-pressure gas through expansion engine:									
Pressure in, atm.	300	189	350*	162	145	130	120	27.5	23
Pressure out, atm.	10	10	37*	37	2	7.6	10	1.5	1.14
Temp. out, °K.	108	108	133*	133	22.9	29.6	31.3	5.9	4.36
Flash tank pressures, atm.	10	10	1.2	1.2	2	2	2	1.5	1.14
atm.	1.2	1.2			1	1	1	1	1
% of high-pressure gas through expansion engine	57	60	30	38	66	60	56	43	49
% of high-pressure gas liquefied	28.8	25.7	41.5	31.5	31.1	29.3	30.3	34.4	46.2
Carnot power, kw./100 std. cu. ft./hr. liquefied:									
To cool to precool temp. at 1 atm.	0.008	0.014	0.030	0.042	0.163	0.20	0.22	0.434	0.480
To liquefy, from precool temp.	0.680	0.674	0.658	0.646	0.777	0.74	0.72	0.436	0.390
Total	0.688	0.688	0.688	0.688	0.940	0.940	0.940	0.870	0.870
Actual power, kw./100 std. cu. ft./hr. liquefied:									
Precooling	0.04	0.07	0.20	0.36	0.93	1.05	1.10	2.61	2.96
Gas compression at 77% efficiency	1.90	1.89	1.78	1.58	2.03	1.65	1.60	1.44	0.96
Power return from expanders	—0.17	—0.16	—0.08	—0.03	—0.06	—0.04	—0.03	—0.005	—0.003
Plant auxiliary power except precooling	0.17	0.19	0.12	0.16	0.16	0.17	0.16	0.14	0.11
Total	1.94	1.99	2.02	2.07	3.06	2.83	2.83	4.19	4.03
% Carnot efficiency	35.5	34.5	34.0	33.2	30.7	33.2	33.2	20.8	21.6

---

* Followed by reheat and turbo-expander expansion. 180°K. and 37 atm. in, 1.2 atm. and 83° K. out.

The engine expansion commences at the precool temperature in all cases shown here.

NOTE: kw. hr./100 std. cu. ft. is the same as kw./100 std. cu. ft./hr. It may be regarded as energy per unit of product or as power per unit rate of production. We refer to it herein as power, following the convention in the industry, and it is ordinarily expressed as kw. hr./100 std. cu. ft.

down and liquefaction as the total heat removed. In the case of air cooling and liquefaction, the Carnot work is only 1.75 times as much as the total heat removed.

ACTUAL POWER REQUIREMENTS FOR LIQUEFACTION

Based on the general principles of liquefaction with minimum power consumption that are stated in the first paragraph of the section herein on Joule-Thomson refrigeration, based on the authors' experience in designing and optimizing of air separation and liquefaction plants of very large size, and based on the similarity of the problems of liquefaction of air, hydrogen, and helium on a large scale, the authors have calculated several different cycles for liquefaction of air, hydrogen, and helium.

Pressure ratios of 2.8 for each stage are generally used, commencing each stage of compression at 100°F. and using 77% adiabatic efficiency of compression including motor efficiency. Expansion engines and turbo-expanders are assumed to be 77% adiabatic efficient, with expansion commencing at the precool temperature and in nearly all cases extending to saturation. It is found that reheat and further expansion in a turbo-expander is undesirable from the standpoint of minimum power. For the large expansion engines that are considered, 93% of the energy removed from the gas in the expander is assumed to be recovered and returned into the electrical system by means of the generators used as power absorbers, or recovered by direct mechanical conversion.

Temperature differences in heat exchangers are in general based on being 0.036 times the absolute temperature at each end. This fixes the percentage of the high-pressure gas that must be bypassed around the main heat exchanger through the expansion engine. Heat leak above the 64°, 69°, or 80°K. level is allowed for in the amount to be expected in a 200 ton/day size of air separation and liquefaction plant, specifically 26 B.t.u./lb. mole (387 std. cu. ft.) of gas compressed, based on experience with a wide range of plant sizes over many years. With the assumption of the use of vacuum powder insulation, such as has been used widely since it was reported by Dewar (*4*) in 1898, and other means of vacuum insulation with radiation shielding, heat leak from the temperature level of liquid hydrogen up to liquid nitrogen temperature is allowed for at the rate of 0.7 B.t.u./lb. mole of gas compressed. Heat leak of 0.26 B.t.u./lb. mole of gas compressed is allowed for below liquid hydrogen precool temperature.

In the case of air liquefaction, the liquid air is considered to be withdrawn at 83°K. (—190°C. or —310°F.), a temperature to which liquid oxygen and liquid nitrogen can be conveniently cooled and commonly are cooled in efficient air separation and liquefaction plants. This is a little warmer than liquid air at its atmospheric pressure boiling point.

Plant auxiliary power requirements for heaters, blowers, motor-generator sets, cooling tower pumps and fans, etc., are allowed for to the extent of 3.6% to 10% of the total power consumption on the basis of the same allowance for auxiliary power per std. cu. ft./hr. of gas compressed as in a 200 ton/day air separation and liquefaction plant, namely 0.19 kw./lb. mole/hr. (387 std. cu. ft./hr.) of gas compression.

Table 1 shows the basic characteristics of the liquefaction processes for air, hydrogen, and helium that were computed and the breakdown of the computed power requirements. Also for each case, the Carnot power requirement for cooling the gas at atmospheric pressure to the precool temperature is tabulated, as is the Carnot power requirement for the remainder of the cooling to liquefaction, including in the case of hydrogen the power for ortho to para conversion. The total Carnot power requirement is also tabulated. The percentage of Carnot efficiency, which is tabulated, is the total Carnot (minimum) power divided by the total actual power computed.

The power was calculated for precooling air to various temperatures, hydrogen to 69°K., and helium to 14°K. This includes the power for compression of gases used as precoolants; that is, Freon and nitrogen for precooling hydrogen, and Freon, nitrogen, and hydrogen for precooling helium. This also includes the vacuum-pumping of nitrogen and hydrogen precoolants. Allowance was made for power return from the expansion engines for nitrogen and hydrogen precoolants. Plant auxiliary power requirements relating to precoolants were included on the basis of the aforementioned 0.19 kw. per 387 std. cu. ft./hr. of precoolant gas compression. From calculations for these cases, the actual precooling power for the remaining cases in the table were estimated, including hydrogen precooled to 80°K. and 64°K., and helium precooled to 11°K. The heat that must be removed in precooling equals the sensible heat in cooling at atmospheric pressure of the gas to be liquefied, plus the increase in Joule-Thomson refrigeration of all the gas compressed at its actual high pressure, in cooling it from the sink temperature to the precool temperature.

The actual heat removed in precooling also includes the heat leak into the system above the precool temperature, plus any warm-end temperature-difference refrigeration loss from the heat exchange system at sink temperature in excess of the loss from the warm end of the main heat exchanger at precool temperature. This includes the refrigeration loss in any vacuum-pumped precoolant gas that is vented cold. In addition to these first law losses in precooling, there are the second law losses owing to the existence of temperature differences throughout the precooling heat exchange system. First law losses in precooling also include refrigeration requirements for dryers and other adsorption or absorption purifiers and for their regeneration and subsequent cool-down.

The various processes compared in Table 1 give a power comparison among different precool temperature levels. For air, a wide range of high pressures is compared. For hydrogen and helium, pressures close to the inversion pressures are used. In all cases, engine expansion is carried out for part of the high-pressure gas, from the precool temperature and pressure down to saturation temperature and pressure, based on 77% adiabatic efficiency. One exception is helium at 14°K. for which the expansion starts at 27.5 atm. and ends at 1.5 atm. and 5.9°K., still 1.2°C. warmer than saturation. Deeper precooling of helium than to the hydrogen triple point would be necessary in order to be able to expand helium in an engine down to saturation.

In the case of air expansion from 189°K. (−120°F.) and 350 atm. (5,140 lb./sq. in. gauge) to the critical point of air at 37 atm., the computation is with 47°C. of reheat followed by a turbo-expander expansion to 1.2 atm. and saturation. This case is inferior in power consumption, however, to other cases shown in which the exhaust air from the initial expander is warmed and returned to the compressor at 10 or 37 atm. rather than being expanded on down to low pressure in a turbo-expander after reheat.

It appears that the lowest power consumption in air liquefaction may be obtained with extremely deep precooling with Freon 13 or with extremely high pressure, in both cases having substantial back-pressure on the expansion engine so that this fraction of the air is recycled at an interstage pressure. A flash tank at 10 to 20 atm. is also required.

For hydrogen, the case in which expansion commences at 80°K. and 145 atm. and goes to 2 atm. involves too high a pressure ratio to be carried out economically in a single-stage reciprocating expander. This would have to be divided into two stages without reheat between, the second stage taking place in a turbo-expander.

The lowest power consumption that was calculated for hydrogen was with a moderate degree of vacuum-pumping of nitrogen precoolant, to precool to 69°K. The same total power figure was computed also with vacuum-pumping to the nitrogen triple point, precooling to 64°K. All cases computed for hydrogen use continuous equilibrium ortho to para conversion of the hydrogen to be liquefied, during its cool-down.

For helium, the inlet pressure of the expander is low enough (staying under the inversion pressure) to permit using turbo-expanders in all cases. The pressure ratio is high enough for it to be desirable to use two stages of turbo-expanders, without reheat between stages.

The lowest power consumption for helium is calculated to be achieved with vacuum-pumping of solid hydrogen to 11°K. rather than only to 14°K. at the hydrogen triple point. However, it is doubted that it is mechanically feasible to vacuum-pump solid hydrogen in a continuous process. Liquid hydrogen used for precooling helium should not have been converted to para, because this would be a waste of refrigeration.

It is noteworthy that for the cases that were calculated and are compared in Table 1, the power requirement for liquefying air or hydrogen or helium is generally not affected greatly by the particular precool temperature chosen since deeper precooling is generally accompanied by fewer stages of compression.

For hydrogen and especially for helium, it is necessary to build-in pressure drop for the high-pressure gas in the main heat exchanger paralleling the expander, so that the gas will emerge from the cold end of the heat exchanger and before the expansion valve at low enough pressure to obtain minimum enthalpy at the temperature the heat exchanger and plant are designed to reach; that is, so as not to cross over the inversion curve during the cool-down.

In Table 1, the cases for hydrogen and helium all have flash tanks at 1 atm. that require vacuum-pumping of the small amount of flash gas in order to get it back through the main heat exchanger to the warm end, up to the precool temperature. In all cases calculated, pressure drop through the heat exchangers and other equipment is allowed for.

Actually, air liquefiers are generally associated with air distilling columns, and the total power consumption includes the work of separating the air. Thus the total consumption is likely to be at least as high as 2.8 kw./100 std. cu. ft./hr. of liquid oxygen and nitrogen, rather than 1.9 to 2.0 kw./100 std. cu. ft./hr. of air or nitrogen liquefied without distillation. Thus, this entire analysis of air liquefiers is a somewhat artificial comparison in relation to the normal requirement to include distillation. However, for purposes of comparison with hydrogen and helium liquefaction, it is essential herein to examine liquefaction separate from the other operation of distillation.

CARNOT EFFICIENCIES ACHIEVABLE IN LIQUEFACTION

Figure 8 shows a comparison of the Carnot efficiencies for cool-down and liquefaction of air, hydrogen, and

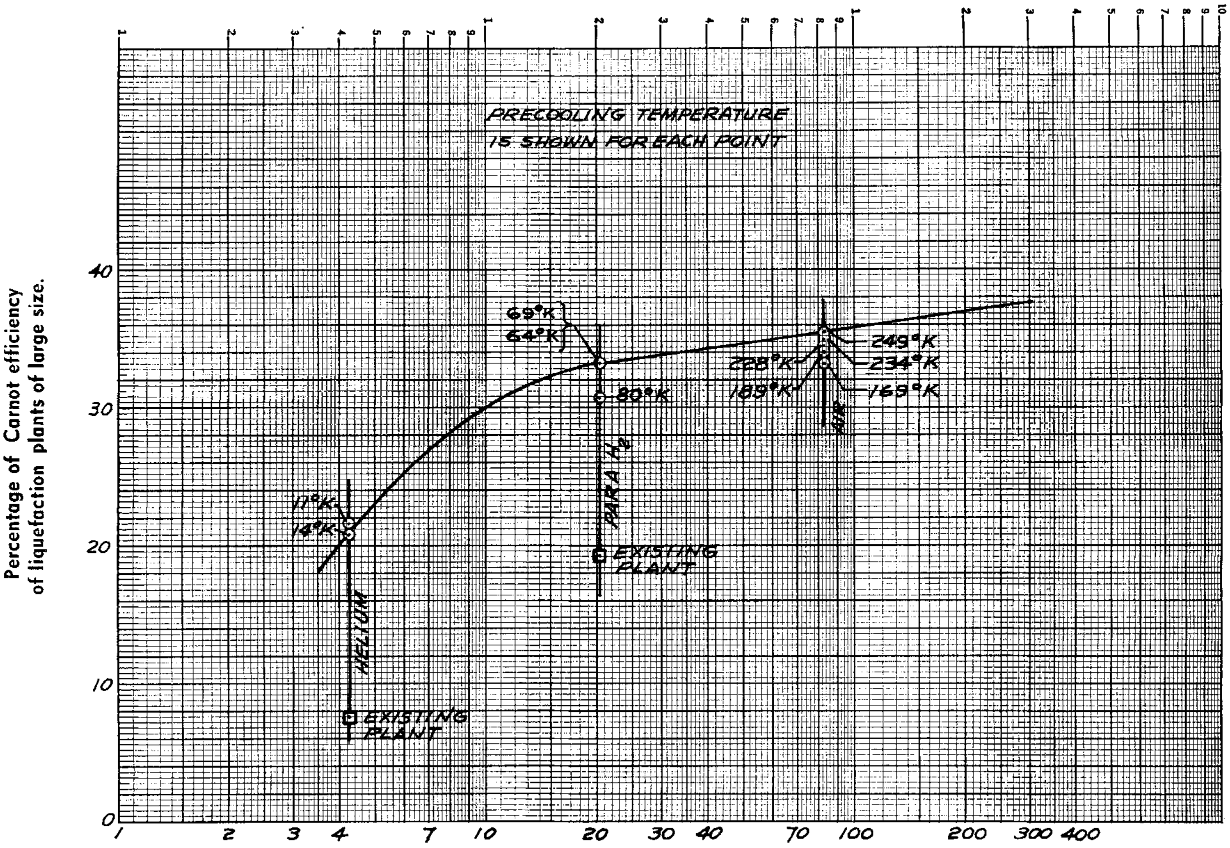

Fig. 8. Efficiency of large liquefaction plants vs. boiling point of liquid.

helium, as arrived at in Table 1, plotted vs. a logarithmic scale of boiling point temperature of each gas. Figure 8 illustrates that 35.5% Carnot efficiency is feasible for air liquefaction, and that at much lower temperature almost as high as an efficiency of 33.2% is achievable for hydrogen conversion and liquefaction, but that at the still lower temperature of helium liquefaction only about 20.8% efficiency is reasonably attainable. We believe our numbers are of the right order of magnitude.

On Figure 8, points are also shown for reported performance of one of the largest helium liquefiers in existence (yet far smaller than the size we envision), and for a large liquid hydrogen plant. These much lower efficiency points demonstrate that the highly efficient very large liquefaction plants aimed toward in this paper will constitute a high degree of technological advancement over any existing plants that the authors know about in detail, especially in the cases of hydrogen and helium.

The helium liquefaction plant represented by the point shown at less than 8% Carnot efficiency, is Collins' 25 to 32 liters/hr. plant at Massachusetts Institute of Technology, Cambridge, Massachusetts, consuming 45 kw. plus liquid nitrogen precoolant (reference *16*, p. 68). This plant does not liquefy hydrogen as precoolant, nor does it liquefy its own nitrogen precoolant with the aid of Freon precooling and a nitrogen expansion engine. Our projected helium liquefier of 21% Carnot efficiency would be of a size using thousands of kw., a size justifying all of these refinements that Collins did not include.

The 19% Carnot efficiency hydrogen liquefaction plant indicated on Figure 8 is the first very large liquid hydrogen plant that was built. It was built in a crash program, and utilized two medium-size existing-design liquid oxygen plants to liquefy the nitrogen precoolant for the hydrogen. It used low-pressure hydrogen turbo-expanders rather than the high-pressure reciprocating expanders now in use. The very large integrated hydrogen liquefiers that the authors envision should achieve the much higher efficiency of 33% that they calculate.

The authors believe that technical developments for hydrogen liquefaction are now moving very rapidly toward these power consumption and efficiency goals.

LITERATURE CITED

1. Collins, S. C., and R. L. Cannaday, "Expansion Machines for Low Temperature Processes," Oxford Univ. Press, London, England (1958).
2. Davies, Mansel, "The Physical Principles of Gas Liquefaction and Low Temperature Rectification," pp. 1-84, 96, 128, 160, 192, Longmans, Green and Co., New York (1949).
3. Davis, Harry M., *Sci. Am.*, pp. 30-39, (June, 1949).
4. Dewar, James, *Proc. Roy. Inst.*, **15**, 824 (1898).
5. Dodge, B. F., "Chemical Engineering Thermodynamics," pp. 417-422, 456-482, McGraw-Hill, New York (1944).
6. Dodge, B. F., J. H. Perry's "Chemical Engineers' Handbook," 3 ed., pp. 1701-1710, McGraw-Hill, New York (1950).
7. Gifford, W. E., "Advances in Cryogenic Engineering," Vol. 2, pp. 1-7, Plenum Press.
8. Intern. Inst. of Refrig., Kamerlingh Onnes Laboratory, Leiden, Netherlands, Charts for Nitrogen (May 1, 1940), Helium (Aug. 15, 1941), Oxygen (Dec. 1, 1942).
9. Johnston, H. L., I. I. Bezman, and C. B. Hood, *J. Am. Chem. Soc.*, 68, 2367-2373 (Nov., 1946).
10. Landsbaum, E. M., W. S. Dodds, W. F. Stevens, B. J. Sollami, and L. F. Stutzman, *A.I.Ch.E. Journal*, **1**, 302-304 (Sept., 1955).

11. Latimer, R. E., *ibid.*, 3, 75-82 (March, 1957).
12. Michels, Wassenaar, and Wolkers, *Appl. Sci. Res. Sect. A.*, 5, Nos. 2-3, pp. 121-136 (1955).
13. Mullins, J. C., W. T. Ziegler, and B. S. Kirk, "The Thermodynamic Properties of Parahydrogen From 1° to 22°K," Eng. Exper. Station, Georgia Inst. of Technol., Atlanta, Georgia (Nov. 1, 1961).
14. Roder, H. M., and R. D. Goodwin, "Tech. Note 130, Provisional Thermodynamic Functions for Para-Hydrogen," Natl. Bur. Stds., Boulder, Colo. (1961).
15. Ruhemann, Martin, "The Separation of Gases," 2 ed., pp. 112-140, 163-172, Oxford Univ. Press, Oxford, England (1949).
16. Scott, Russell B., "Cryogenic Engineering," pp. 7-17, 31-34, 41-50, 53-74, 204, 211-214, 268-321, D. Van Nostrand, New York (1959).
17. Stewart, R. B., R. D. McCarty, L. J. Ericks, R. D. Weekley, Nat. Bur. Stds., Boulder, Colo., Interim Thermodynamic Charts for Para-Hydrogen (1961).
18. Williams, V. C., *Trans. A.I.Ch.E.*, **39**, pp. 93-111 (Feb., 1943).
19. Woolley, H. W., R. B. Scott, and F. G. Brickwedde, *J. Res. Natl. Bur. Stds.*, **41**, Res. paper *RP 1932*, (Nov., 1948).

Manuscript received June 11, 1963; revision received September 30, 1963; paper accepted October 2, 1963.

COMMUNICATIONS TO THE EDITOR

A Novel Technique for Determining Mass Transfer Coefficients in Agitated Solid-Liquid Systems

A. J. MADDEN and D. G. NELSON
University of Minnesota, Minneapolis, Minnesota

In a recent paper Harriott (*4*) has pointed out the marked disagreement in the literature regarding mass transfer coefficients in agitated solid-liquid systems. Widely conflicting claims have been made as to the dependence of particle-fluid mass transfer coefficients upon various operating parameters (impeller speed, particle-fluid density difference, etc.). In part this may be owing to difficulties in obtaining reliable data suggesting the need for an improved experimental method, designed to overcome shortcomings of some of the earlier studies.

METAL-SOLUTION CHEMICAL REACTIONS FOR MASS TRANSFER STUDIES

It has been established that under proper circumstances certain metals will dissolve chemically in aqueous solutions at diffusion-controlled rates. This fact does not appear to be generally appreciated, and the potentialities for studying mass transfer using metal-solution reactions have not been fully exploited. In the application of this idea to studies on mass transfer in agitated solid-liquid systems, the use of a metal as the solid has several obvious advantages. First, the problem of particle attrition should be greatly minimized as compared with studies on crystalline solids, such as salt or boric acid. Second, particle geometry may be more precisely defined, at least under some circumstances. A number of metals and alloys are available as spheres in a wide range of sizes (ball bearings, Linde microspheres), and spherical shapes are also available for a number of other inert, nonmetallic materials (glass beads, plastics). The latter materials may be given a metal surface by various metallizing procedures. By appropriate choice of the substrate particle and regulation of the thickness of applied metal surface, a wide range of effective particle densities may be fabricated. This would make possible a systematic examination of the effect of particle-fluid density difference on the mass transfer coefficient without changing other properties of the solid-liquid system. This has not been possible in prior studies.

It should be noted that some of the advantages of metal-solution systems have been achieved in a different way in other studies. Harriott (*4*) claims to have circumvented the attrition problem, together with good definition of particle geometry, in studies on the neutralization of suspensions of small ion-exchange beads. The proposed metal-solution system, however, offers the additional advantage of a systematic study of the density-difference effect.

EVALUATION OF THE TECHNIQUE

Initial exploratory studies on the use of metal-solution reactions for studies in mass transfer were based upon the work of Gregory and Riddiford (*2*). Their study demonstrated that rotating copper and brass disks dissolve in aqueous potassium dichromate—sulfuric acid solutions at rates which are entirely diffusion-controlled, provided that the acidity is sufficiently high. Dissolution rates in their studies varied as the square root of the rotational speed of the disks, as required by the ex-

(*Continued on page 427*)

D. G. Nelson is with Minnesota Mining and Manufacturing Company, St. Paul, Minnesota.